

# Conformal mapping of some non-harmonic functions in transport theory

BY MARTIN Z. BAZANT

*Department of Mathematics  
Massachusetts Institute of Technology, Cambridge, MA 02139 USA  
and  
École Supérieure de Physique et de Chimie Industrielles  
10 rue Vauquelin, 75231 Paris, France.*

Conformal mapping has been applied mostly to harmonic functions, i.e. solutions of Laplace's equation. In this paper, it is noted that some other equations are also conformally invariant and thus equally well suited for conformal mapping in two dimensions. In physics, these include steady states of various nonlinear diffusion equations, the advection-diffusion equations for potential flows, and the Nernst-Planck equations for electrochemical transport in quasi-neutral or supporting electrolytes. Exact solutions for complicated geometries are obtained by conformal mapping to simple geometries in the usual way. Novel examples include nonlinear advection-diffusion layers around absorbing objects and concentration polarizations in electrochemical cells. Although some of these results could be obtained by other methods (e.g. Boussinesq's streamline coordinates), the present approach is based on a simple unifying principle with more general applicability. It reveals a basic geometrical equivalence of similarity solutions for a broad class of transport processes and paves the way for new applications of conformal mapping, e.g. to non-Laplacian fractal growth.

**Keywords:** conformal mapping, non-harmonic functions, nonlinear diffusion, advection-diffusion, electrochemical transport

## 1. Introduction

Complex analysis is one of the most beautiful subjects in mathematics, and, in spite of involving imaginary numbers, it has remarkable relevance for 'real' applications. One of its most useful techniques is conformal mapping, which transforms planar domains according to analytic functions,  $w = f(z)$ , with  $f'(z) \neq 0$ . Geometrically, such mappings induce upon the plane a uniform, local stretching by  $|f'(z)|$  and a local rotation by  $\arg f'(z)$ . This 'ampli-twist' interpretation of the derivative implies conformality, the preservation of angles between intersecting curves (Needham 1997).

The classical application of conformal mapping is to solve Laplace's equation,

$$\nabla^2 \phi = 0, \quad (1.1)$$

i.e. to determine harmonic functions, in complicated planar domains by mapping to simple domains (Needham 1997; Churchill & Brown 1990; Carrier *et. al.* 1983; Henrici 1986; Trefethen 1986; Batchelor 1967). The method relies on the conformal invariance of Eq. (1.1), which remains the same after a conformal change of variables. Before the advent of computers, important analytical solutions were thus obtained for electric fields in capacitors, thermal fluxes around pipes, inviscid flows past airfoils, etc. (Needham 1997; Churchill & Brown 1990; Batchelor 1967). Today, conformal mapping is still used extensively in numerical methods (Henrici 1986; Trefethen 1986).

Currently in physics, a veritable renaissance in conformal mapping is centering around ‘Laplacian-growth’ phenomena, in which a free boundary moves in proportion to (some power of) the normal derivative of a harmonic function. Continuous problems of this type include viscous fingering, where the pressure is harmonic (Bensimon *et al.* 1986; Saffman 1986), and solidification from a supercooled melt, where the temperature is harmonic in some approximations (Kessler *et al.* 1988; Cummings *et al.* 1999). Such problems can be elegantly formulated in terms of time-dependent conformal maps, which generate the moving boundary from its initial position. This idea was first developed in 1945 in the Russian literature by Polubarinova-Kochina and Galin (Howison 1992), with recent interest in physics stimulated by Shraiman & Bensimon (1984) focusing on the subtle issues of pattern selection and finite-time singularities (Saffman & Taylor 1958; Howison 1986; Tanveer 1987; Dai *et al.* 1991; Ben Amar 1991; Howison 1992; Tanveer 1993; Ben Amar & Brener 1996; Ben Amar & Poiré 1999; Feigenbaum *et al.* 2001).

Stochastic problems of a similar type include diffusion-limited aggregation (DLA) (Witten & Sander 1981) and dielectric breakdown (Niemeyer *et al.* 1984). Recently, Hastings & Levitov (1998) proposed an analogous method to describe DLA using iterated conformal maps, which has stimulated a flurry of activity applying conformal mapping to Laplacian fractal-growth phenomena (Davidovitch *et al.* 1999, 2000; Barra *et al.* 2002a, 2002b; Stepanov & Levitov 2001; Hastings 2001; Somfai *et al.* 1999; Ball & Somfai 2002). One of our motivations here is to extend such powerful analytical methods to other growth phenomena limited by *non-Laplacian* transport, inspired by recent work on dendritic solidification in a flowing melt (Cummings *et al.* 1999) and quasi-static brittle fracture (Barra *et al.* 2002b).

Compared to the vast literature on conformal mapping for Laplace’s equation, the technique has scarcely been applied to any other equations. The difficulty with non-harmonic functions is illustrated by Helmholtz’s equation,

$$\nabla^2 \phi = \phi, \quad (1.2)$$

which arises in transient diffusion and electromagnetic radiation (Morse & Feshbach 1953). After conformal mapping,  $w = f(z)$ , it acquires a cumbersome, non-constant coefficient (the Jacobian of the map),

$$|f'|^2 \nabla^2 \phi = \phi. \quad (1.3)$$

Similarly, the bi-harmonic equation,

$$\nabla^2 \nabla^2 \phi = 0, \quad (1.4)$$

which arises in two-dimensional viscous flows (Batchelor 1967) and elasticity (Muskhelishvili 1953), transforms with an extra Laplacian term (see below),

$$|f'|^4 \nabla^2 \nabla^2 \phi = -4|f''|^2 \nabla^2 \phi. \quad (1.5)$$

In this special case, conformal mapping is commonly used (e.g. Chan *et al.* 1997; Crowdy 1999, 2002; Barra *et al.* 2002b) because solutions can be expressed in terms of analytic functions in Goursat form (Muskhelishvili 1953). Nevertheless, given the singular ease of applying conformal mapping to Laplace's equation, it is natural to ask whether any other equations share its conformal invariance, which is widely believed to be unique.

In this paper, we show that certain *systems* of nonlinear equations, with non-harmonic solutions, are also conformally invariant. In section 2, we give a simple proof of this fact and some of its consequences. In section 3, we discuss applications to nonlinear diffusion phenomena and show that single conformally invariant equations can always be reduced to Laplace's equation (which is not true for coupled systems). In section 4, we apply conformal mapping to linear and nonlinear advection-diffusion in a potential flow, which is equivalent to Boussinesq's streamline coordinates in a special case (Boussinesq 1905). In section 5, we apply conformal mapping to nonlinear electrochemical transport, apparently for the first time. Finally, in section 6, we summarize and briefly discuss further applications to non-Laplacian growth phenomena.

## 2. Mathematical Theory

### (a) Conformal Mapping without Laplace's Equation?

The standard application of conformal mapping is based on the following two facts:

1. Any harmonic function,  $\phi$ , in a singly connected planar domain,  $\Omega_w$ , is the real part of a analytic function,  $\Phi$ , the 'complex potential' (which is unique up to an additive constant):  $\phi = \operatorname{Re} \Phi(w)$ .
2. Since analyticity is preserved under composition, harmonicity is preserved under conformal mapping, so  $\phi = \operatorname{Re} \Phi(f(z))$  is harmonic in  $\Omega_z = f^{-1}(\Omega_w)$ .

Presented like this, it seems that conformal mapping is closely tied to harmonic functions, but Fact 2 simply expresses the conformal invariance of Laplace's equation: A solution,  $\phi(w)$ , is the same in any mapped coordinate system,  $\phi(f(z))$ . Fact 1, a special relation between harmonic functions and analytic functions, is not really needed. If another equation were also conformally invariant, then its non-harmonic solutions,  $\phi(w, \bar{w})$ , would be preserved under conformal mapping in the same way,  $\phi(f(z), f(\bar{z}))$ . (See Fig. 1.)

### (b) Transformations of Differential Operators

In order to seek such non-Laplacian invariant equations, we review the transformation properties of some basic differential operators. Following Argand and Gauss, it is convenient to represent two-dimensional vectors,  $\mathbf{a} = a_x \hat{\mathbf{x}} + a_y \hat{\mathbf{y}}$ , as complex

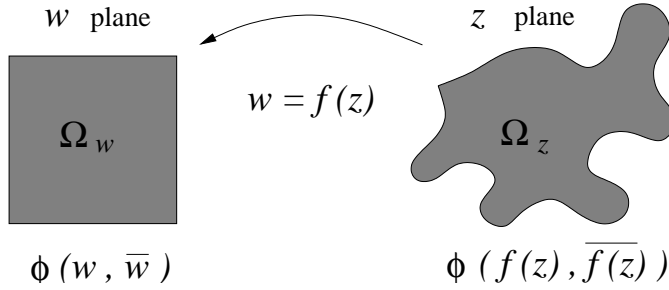


Figure 1. Conformal mapping,  $w = f(z)$ , of a solution,  $\phi$ , to a conformally invariant equation from a complicated domain,  $\Omega_z$ , and a simple domain,  $\Omega_w$ .

numbers,  $a = a_x + a_y i$ . We thus express the gradient vector operator in the plane as a complex scalar operator,

$$\nabla = \hat{x} \frac{\partial}{\partial x} + \hat{y} \frac{\partial}{\partial y} \quad \longleftrightarrow \quad \nabla = \frac{\partial}{\partial x} + i \frac{\partial}{\partial y}. \quad (2.1)$$

The complex gradient has the essential property that  $\nabla f = 0$  if and only if  $f$  is analytic, in which case,  $\bar{\nabla} f = 2f'$  (Needham 1997). Since  $\mathbf{a} \cdot \mathbf{b} = \operatorname{Re} a\bar{b}$ , the Laplacian operator can be expressed as,

$$\nabla \cdot \nabla = \operatorname{Re} \nabla \bar{\nabla} = \nabla \bar{\nabla}, \quad (2.2)$$

(if mixed partial derivatives can be taken in any order). Similarly, the ‘advection operator’, which acts on *two* real functions  $\phi$  and  $c$ , takes the form,

$$\nabla \phi \cdot \nabla c = \operatorname{Re} (\nabla \phi) \bar{\nabla} c. \quad (2.3)$$

Under a conformal mapping,  $w = f(z)$ , the gradient transforms as,

$$\nabla_z = \bar{f}' \nabla_w. \quad (2.4)$$

This basic fact, combining the ampli-twist property and the chain rule, makes it easy to transform differential operators (Needham 1997). The Laplacian transforms as,

$$\nabla_z \bar{\nabla}_z = (\nabla_z f') \bar{\nabla}_w + |f'|^2 \nabla_w \bar{\nabla}_w = |f'|^2 \nabla_w \bar{\nabla}_w \quad (2.5)$$

where  $\nabla_z f' = 0$  because  $f'$  is also analytic. This immediately implies the conformal invariance of Laplace’s equation (2.5), and the non-invariance of Helmholtz’s equation (1.2). We can also easily transform the bi-harmonic equation (1.4) as in Eq. (1.5) with the help of an identity,  $\Delta|f|^2 = 4|f'|^2$ , of Needham (1997) applied to  $f'$ .

Everything in this paper follows from the simple observation that the advection operator transforms just like the Laplacian,

$$\operatorname{Re} (\nabla_z \phi) \bar{\nabla}_z c = |f'|^2 \operatorname{Re} (\nabla_w \phi) \bar{\nabla}_w c. \quad (2.6)$$

Each operator involves a ‘dot product of two gradients’, so the same Jacobian factor,  $|f'|^2$ , appears in both cases, as a result of Eq. (2.4). The transformation laws, Eq. (2.5) and Eq. (2.6), are surely well known, but it seems that some general implications have been overlooked, or at least not fully exploited in physical applications.

(c) *Conformally Invariant Equations*

The identities (2.5) and (2.6) imply the conformal invariance of any system of equations of the general form,

$$\sum_{i=1}^N \left( a_i(\phi) \nabla^2 \phi_i + \sum_{j=i}^N a_{ij}(\phi) \nabla \phi_i \cdot \nabla \phi_j \right) = 0 \quad (2.7)$$

where the coefficients  $a_i(\phi)$  and  $a_{ij}(\phi)$  may be nonlinear functions of the unknowns,  $\phi = (\phi_1, \phi_2, \dots, \phi_N)$ , but not of the independent variables or any derivatives of the unknowns. Thus we arrive at our main result:

**Theorem 2.1.** (Conformal Mapping Theorem.) *Let  $\phi(w, \bar{w})$  satisfy Eq. (2.7) in a domain  $\Omega_w$  and  $w = f(z)$  be a conformal mapping from  $\Omega_z$  to  $\Omega_w$ . Then  $\phi(f(z), \bar{f(z)})$  satisfies Eq. (2.7) in  $\Omega_z$ .*

(d) *Conformally Invariant Boundary Conditions*

Conformal mapping is most useful when the boundary conditions are also invariant. Dirichlet ( $\phi_i = \text{constant}$ ) or Neumann ( $\hat{\mathbf{n}} \cdot \nabla \phi_i = 0$ ) conditions are typically assumed, but here we consider the straight-forward generalizations,

$$b_i(\phi) = 0 \quad \text{and} \quad \sum_{j=1}^N b_{ij}(\phi) (\hat{\mathbf{n}} \cdot \nabla \phi_j)^{\alpha_i} = 0 \quad (2.8)$$

respectively, where  $b_i(\phi)$  and  $b_{ij}(\phi)$  are nonlinear functions of the unknowns,  $\alpha_i$  is a constant, and  $\hat{\mathbf{n}}$  is the unit normal. The conformal invariance of the former is obvious, so we focus briefly on the latter.

It is convenient to locally transform a vector field,  $F$ , along a given contour as,  $\tilde{F} = t \bar{F}$ , so that  $\text{Re } \tilde{F}$  and  $\text{Im } \tilde{F}$  are the projections onto the unit tangent,  $t = dz/|dz|$ , and the (right-handed) unit normal,  $n = -it$ , respectively. Since the tangent transforms as,  $t_w = t_z f'/|f'|$ , and the gradient as,  $\nabla_z = \bar{f}' \nabla_w$ , we find,  $\tilde{\nabla}_z = |f'| \tilde{\nabla}_w$ . The invariance of Eq. (2.8) follows after taking the imaginary part on the boundary contour.

(e) *Gradient-Driven Flux Densities*

Generalizing  $\nabla \phi$  for Laplacian problems, we define a ‘flux density’ for solutions of Eq. (2.7) to be any quasi-linear combination of gradients,

$$\mathbf{F}_i = \sum_{j=1}^N c_{ij}(\phi) \nabla \phi_j, \quad (2.9)$$

where  $c_{ij}(\phi)$  are nonlinear functions. The transformation rules above for the gradient apply more generally to any flux density,

$$F_z = \bar{f}' F_w \quad \text{and} \quad \tilde{F}_z = |f'| \tilde{F}_w. \quad (2.10)$$

These basic identities imply a curious geometrical equivalence between solutions to *different* conformally invariant systems:

**Theorem 2.2.** (Equivalence Theorem.) *Let  $\phi^{(1)}$  and  $\phi^{(2)}$  satisfy equations of the form (2.7) with corresponding flux densities,  $F^{(1)}$  and  $F^{(2)}$ , of the form (2.9). If  $F_z^{(1)} = a F_z^{(2)}$  on a contour  $C_z$  for some complex constant  $a$ , then  $F_w^{(1)} = a F_w^{(2)}$  on the image,  $C_w = f(C_z)$ , after a conformal mapping,  $w = f(z)$ .*

An important corollary pertains to ‘similarity solutions’ of Eqs. (2.7) and (2.8) in which certain variables  $\{\phi_i\}$  involved in a flux density depend on only one Cartesian coordinate, say  $\text{Re } w$ , after conformal mapping,

$$\phi_i = G_i(\text{Re } f(z)). \quad (2.11)$$

(Our examples below are mostly of this type.) Such special solutions share the same flux lines (level curves of  $\text{Im } f(z)$ ) and iso-potentials (level curves of  $\text{Re } f(z)$ ) in any geometry attainable by conformal mapping. They also share the same *spatial distribution* of flux density on an iso-potential, although the *magnitudes* generally differ.

#### (f) Flux Integrals

An important physical quantity is the total normal flux through a contour,  $\text{Nu}(C)$ , sometimes called the ‘Nusselt number’. For any contour,  $C$ , we define a complex total flux,

$$I(C) = \int_C \tilde{F} |dz| = \int_C \overline{F} dz, \quad (2.12)$$

such that  $\text{Re } I(C)$  is the integrated tangential flux and  $\text{Im } I(C) = \text{Nu}(C)$ . From Eq. (2.10) and  $dw = f' dz$ , we conclude,  $I(C_z) = I(C_w)$ . Therefore, flux integrals can be calculated in any convenient geometry, which has useful applications.

For example, if  $\tilde{F}_w$  is constant on a contour  $C_w = f(C_z)$ , then for any conformal mapping, we have,  $I(C_z) = I(C_w) = \ell(C_w) \tilde{F}_w$ , where  $\ell(C_w)$  is simply the length of  $C_w$ . In the case of gradient fluxes for harmonic functions, this is the basis for the method of iterated conformal maps for DLA, in which the ‘harmonic measure’ for random growth events on a fractal cluster is replaced by a uniform probability measure on the unit circle (Hastings & Levitov 1998). More generally, a *non-harmonic* probability measure for fractal growth can be constructed for any flux law of the form (2.9) for fields satisfying Eq. (2.7).

### 3. Physical Applications to Diffusion Phenomena

Conformally invariant boundary-value problems, Eqs. (2.7) and (2.8), commonly arise in physics from steady conservation laws,

$$\frac{\partial c_i}{\partial t} = \nabla \cdot \mathbf{F}_i = 0, \quad (3.1)$$

for gradient-driven flux densities, Eq. (2.9), with algebraic or zero-flux ( $\hat{\mathbf{n}} \cdot \mathbf{F}_i = 0$ ) boundary conditions, where  $c_i$  is the concentration and  $\mathbf{F}_i$  the flux of substance  $i$ . Hereafter, we focus on flux densities of the form,

$$\mathbf{F}_i = c_i \mathbf{u}_i - D_i(c_i) \nabla c_i, \quad \mathbf{u}_i \propto \nabla \phi \quad (3.2)$$

where  $D_i(c_i)$  is a nonlinear diffusivity,  $\mathbf{u}_i$  is an irrotational vector field causing advection, and  $\phi$  is a (possibly non-harmonic) potential. This class of transport processes includes steady nonlinear advection-diffusion in potential flows, as well as various case of ion transport in electrochemical cells.

Before discussing these cases of coupled dependent variables below, it is instructive to consider nonlinear diffusion in only one variable. The most general equation of the type (2.7) for one variable is,

$$a(c) \nabla^2 c = |\nabla c|^2. \quad (3.3)$$

This equation arises in the Stefan problem of dendritic solidification, where  $c$  is the dimensionless temperature of a supercooled melt and  $a(c)$  is Ivantsov's function, which implicitly determines the position of the liquid-solid interface via  $a(c) = 1$  (Ivantsov 1947). In two dimensions, Bedia & Ben Amar (1994) prove the conformal invariance of Eq. (3.3) and then study similarity solutions,  $c(\xi, \eta) = G(\eta)$ , by conformal mapping,  $w = \xi + i\eta$ , to a plane of parallel flux lines,

$$a(G) G'' = (G')^2, \quad (3.4)$$

where an ordinary differential equation is solved.

More generally, reversing these steps, it is straight-forward to show that any monotonic solution of Eq. (3.4) produces a nonlinear transformation,  $c = G(\phi)$ , from Eq. (3.3) to Laplace's equation (1.1), which implies conformal invariance. There are several famous examples. For steady concentration-dependent diffusion,

$$\nabla \cdot (D(c) \nabla c) = 0, \quad (3.5)$$

it is Kirchhoff's transformation (Kirchhoff 1894; Crank 1975),

$$\phi = G^{-1}(c) = \int_0^c D(x) dx. \quad (3.6)$$

For the (steady or unsteady) Burgers' equation (Whitham 1974),

$$\frac{\partial \mathbf{u}}{\partial t} + \lambda \mathbf{u} \cdot \nabla \mathbf{u} = \nu \nabla^2 \mathbf{u}, \quad (3.7)$$

in an irrotational flow,  $\mathbf{u} = -\nabla h$ , which is equivalent to the KPZ equation without noise (Kardar *et al.* 1986; Medina *et al.* 1989),

$$\frac{\partial h}{\partial t} = \nu \nabla^2 h + \frac{\lambda}{2} |\nabla h|^2 \quad (3.8)$$

it is the Cole-Hopf transformation (Cole 1951; Hopf 1950),

$$\phi = G^{-1}(h) = e^{\lambda h / 2\nu} \quad (3.9)$$

which yields the linear diffusion equation,

$$\frac{\partial \phi}{\partial t} = \nu \nabla^2 \phi \quad (3.10)$$

and thus again Laplace's equation in steady state.

In summary, the general solutions to Equation (3.3) are simply nonlinear functions of harmonic functions, so, in the case of one variable, our theorems can be easily understood in terms of standard conformal mapping. For two or more coupled variables, however, this is no longer true, except for special similarity solutions (as described above). The following sections discuss some truly non-Laplacian physical problems.

## 4. Advection-Diffusion

### (a) Steady Advection-Diffusion in a Potential Flow

Consider the steady diffusion of particles or heat passively advected in a potential flow (Leal 1992; Redner 2001), also allowing for a nonlinear concentration-dependent diffusivity. For a characteristic length,  $L$ , speed,  $U$ , concentration,  $C$ , and diffusivity,  $D(C)$ , the dimensionless, conformally invariant equations are

$$\nabla^2 \phi = 0 \quad \text{and} \quad \text{Pe} \nabla \phi \cdot \nabla c = \nabla \cdot (b(c) \nabla c) \quad (4.1)$$

where  $\phi$  is the velocity potential (scaled to  $UL$ ),  $c$  is the concentration (scaled to  $C$ ),  $b(c)$  is the dimensionless diffusivity, and  $\text{Pe} = UL/D$  is the Péclet number. The latter equation is a steady conservation law for the dimensionless flux density,

$$\mathbf{F} = \text{Pe} c \nabla \phi - b(c) \nabla c \quad (4.2)$$

(scaled to  $DC/L$ ). For  $b(c) = 1$ , these classical equations have been studied recently, e.g. in the contexts of tracer dispersion in porous media (Koplik *et al.* 1994, 1995), vorticity diffusion in strained wakes (Eames & Bush 1999; Hunt & Eames 2002), thermal diffusion (Morega & Behan 1994; Sen & Yang 2000), and dendritic solidification in flowing melts (Kornev & Mukhamadullina 1994; Cummings *et al.* 1999).

### (b) A Class of Similarity Solutions

We begin by reviewing the derivation of a well known similarity solution in the upper half plane,  $w = \xi + i\eta$  ( $\eta > 0$ ), which we can then map to other geometries. As shown in the top left panel of Fig. 2, we consider a straining velocity field,

$$\phi = \text{Re} \Phi, \quad \Phi = w^2, \quad u = \overline{\Phi'} = 2\overline{w} = 2\xi - 2i\eta, \quad (4.3)$$

which advects a concentrated fluid,  $c(\xi, \infty) = 1$ , toward an absorbing wall on the real axis,  $c(\xi, 0) = 0$ . Since the  $\eta$ -component of the velocity (toward the wall) is independent of  $\xi$ , as are the boundary conditions, the concentration depends only on  $\eta$ . The scaling function,

$$c(\xi, \eta; \text{Pe}) = S(\sqrt{\text{Pe}} \eta) = S(\tilde{\eta}), \quad (4.4)$$

satisfies the ordinary boundary-value problem,

$$-2\tilde{\eta} S' = (b(S) S')', \quad S(0) = 0, \quad S(\infty) = 1, \quad (4.5)$$

which is straightforward to solve, at least numerically, for any physical choice of  $b(S)$ . In the presence of advection ( $\text{Pe} > 0$ ), Kirchoff's transformation, Eq. (3.6), unfortunately does not remove the nonlinearity in Eqs. (4.1) and (4.5).

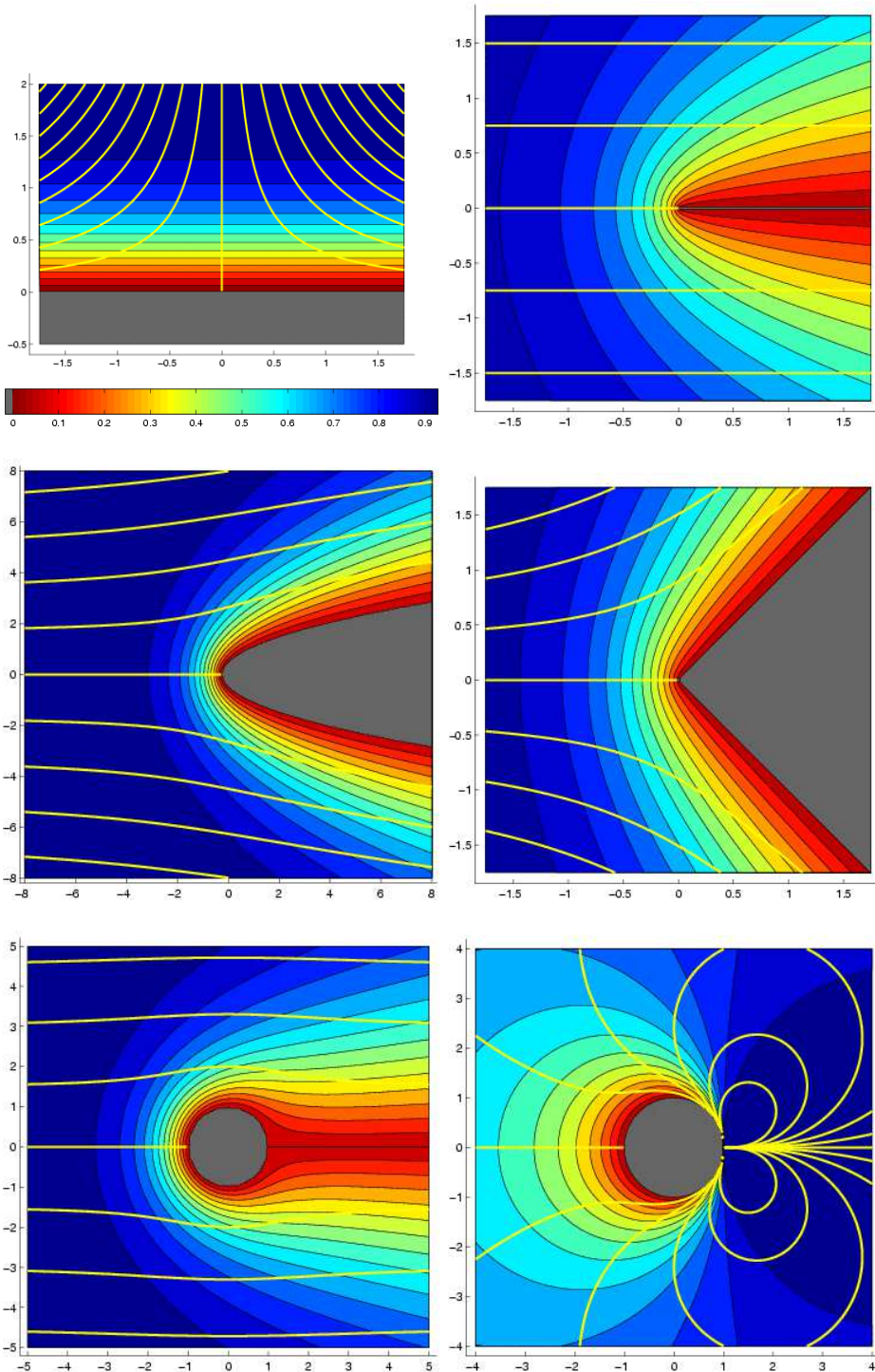


Figure 2. Concentration profiles (contour plots) and potential-flow streamlines (yellow) for steady, linear advection-diffusion layers around various absorbing surfaces (gray) at  $\text{Pe} = 1$ . All solutions are given by Eq. (4.7), where  $w = f(z)$  is a conformal map to the upper half plane (top left). The color scale applies to all panels in Figs. 2 and 3.

Article submitted on 15 January 2003

For a linear diffusivity,  $b(S) = 1$ , Equation (4.5) has a simple, analytical solution (e.g. Cummings *et al.* 1999),

$$S(\tilde{\eta}) = \operatorname{erf}(\tilde{\eta}). \quad (4.6)$$

If extended to the entire  $w$ -plane, where two fluids of different concentrations flow towards each other, this is equivalent to Burgers' solution for a stationary vortex sheet under uniform strain (Burgers 1948). In that case,  $(\phi_\xi, \phi_\eta, c)$  is a three-dimensional velocity field satisfying the Navier-Stokes equations, and  $\text{Pe}$  is the Reynolds number. Inserting a boundary, such as the stationary wall on the real axis, is not consistent with Burgers' solution, however, because the no-slip condition cannot be satisfied. The wall is crucial for conformal mapping to other geometries because it enables us to hide singularities in the lower half plane.

From the solution to Eq. (4.5), for every conformal map to the upper half plane,  $w = f(z)$ , we obtain another similarity solution,

$$\phi = \operatorname{Re} f(z)^2 \quad \text{and} \quad c = S\left(\sqrt{\text{Pe}} \operatorname{Im} f(z)\right) \quad \text{for } \operatorname{Im} f(z) \geq 0 \quad (4.7)$$

which describes the nonlinear advection-diffusion layer in a potential flow of concentrated fluid past the 'leading edge' of an absorbing object. Upstream of the stagnation point,  $f^{-1}(0)$ , the layer's width is  $O(1/\sqrt{\text{Pe}})$ , consistent with simple scaling arguments (Leal 1992). For a linear diffusivity, Eq. (4.6), examples of six different conformal mappings in Eq. (4.7) are shown in Fig. 2 and discussed in detail below, but first we consider some general features of this class of solutions.

### (c) Equivalence of Flux Lines with Linear Diffusion

The flux density for the class of similarity solutions in Eq. (4.7) is easily calculated in the  $w$ -plane and then mapped to the  $z$ -plane using Eq. (2.10). The result is

$$F_z = 2 \overline{f'(z)f(z)} \text{Pe} S\left(\sqrt{\text{Pe}} \operatorname{Im} f(z)\right) - \overline{f'(z)} \sqrt{\text{Pe}} S'\left(\sqrt{\text{Pe}} \operatorname{Im} f(z)\right) \quad (4.8)$$

where the first term describes advection and the second, diffusion. The lines of advective and diffusive flux, which are level curves of  $\operatorname{Im} f(z)^2$  (streamlines) and  $\operatorname{Re} f(z)$ , respectively, are independent of  $\text{Pe}$  and  $b(c)$ , as required by the Equivalence Theorem. In particular, *the diffusive flux lines have the same shape for any flow speed or nonlinear diffusivity* as in the case of simple linear diffusion ( $\text{Pe} = 0$ ,  $b(c) = 1$ ), where  $c \propto \operatorname{Im} f(z)$ , even though advection and nonlinearity obviously both alter the lines of total flux.

The lines of total flux, called 'heatlines' in thermal advection-diffusion, are level curves of the 'heat function' (Kimura & Bejan 1983), which we define in complex notation via  $\nabla H = iF$ . For a linear diffusivity, by comparing with

$$F_z = 2 \overline{f'(z)} \left[ \text{Pe} \overline{f(z)} \operatorname{erf}\left(\sqrt{\text{Pe}} \operatorname{Im} f(z)\right) - i \sqrt{\frac{\text{Pe}}{\pi}} \exp(-\text{Pe} (\operatorname{Im} f(z))^2) \right] \quad (4.9)$$

and integrating, we obtain the heat function for any geometry produced by conformal mapping,

$$H = 2 \operatorname{Re} f(z) \left[ \operatorname{Pe} (\operatorname{Im} f(z)) \operatorname{erf} \left( \sqrt{\operatorname{Pe}} \operatorname{Im} f(z) \right) + \sqrt{\frac{\operatorname{Pe}}{\pi}} \exp(-\operatorname{Pe} (\operatorname{Im} f(z))^2) \right]. \quad (4.10)$$

This result shows how the total-flux lines cross over smoothly from fluid streamlines outside the diffusion layer ( $H \sim \operatorname{Pe} \operatorname{Im} f(z)^2$ ,  $\operatorname{Im} f(z) \gg 1$ ) to diffusive-flux lines near the absorbing surface ( $H \sim 2\sqrt{\operatorname{Pe}/\pi} \operatorname{Re} f(z)$ ,  $\operatorname{Im} f(z) \ll 1$ ).

Sen & Yang (2000) have recently shown that the heat function satisfies Laplace's equation in certain potential-dependent coordinates,

$$\tilde{\nabla}^2 H = 0 \quad \text{where } \tilde{\nabla} \equiv e^{-\operatorname{Pe} \phi} \nabla. \quad (4.11)$$

Although this gives further insight into the mathematical structure of Eq. (4.1), it does not provide a basis for conformal mapping because the coordinate transformation in Eq. (4.11) is not analytic. Moreover, determining the boundary conditions on  $H$  for a given boundary-value problem (4.1) requires knowing the solution  $(\phi, c)$  in advance. For example, on a surface where the concentration is specified, the unknown flux would also be required. These difficulties underscore the fact that the solutions of Eq. (4.1) are fundamentally non-harmonic, even with a linear diffusivity.

On the absorbing surface,  $\operatorname{Im} f(z) = 0$ , the flux density is purely diffusive and in the normal direction. Its spatial distribution is determined *geometrically* via the conformal mapping,

$$|F_z| = \sqrt{\operatorname{Pe}} S'(0) |f'(z)| \quad \text{on } \operatorname{Im} f(z) = 0, \quad (4.12)$$

and only its magnitude depends on  $\operatorname{Pe}$ . (For a linear diffusivity, we have  $S'(0) = 2/\sqrt{\pi}$ .) As explained above, this special property of similarity solutions is predicted by the Equivalence Theorem, not only for advection-diffusion in a potential flow, but also for any other conformally invariant process (e.g. electrochemical transport).

What appears to be the first and only result of this kind is due to Koplik *et al.* (1994, 1995) in the context of tracer dispersion by linear advection-diffusion in porous media. For the special case of potential flow from a dipole source to an equipotential absorbing sink, they prove that the spatial distribution of surface flux (related to the distribution of collected tracer) is independent of  $\operatorname{Pe}$ . In that class of problems the fluxes due to advection and diffusion are always parallel. The present analysis shows that the same conclusion holds for all similarity solutions to Eq. (4.1), even if (i) the two fluxes are not parallel or (ii) the diffusivity is a nonlinear function of the concentration.

#### (d) Streamline Coordinates

In proving their equivalence theorem, Koplik *et al.* (1994, 1995) transform the steady advection-diffusion equation for a potential flow, Eq. (4.1), in the linear case,  $b(c) = 1$ , to 'streamline coordinates',

$$\operatorname{Pe} c_\phi = c_{\phi\phi} + c_{\psi\phi}, \quad (4.13)$$

where  $\Phi = \phi + i\psi$  is the complex potential,  $\phi$ , the velocity potential, and  $\psi$ , the streamfunction. The physical interpretation of Eq. (4.13) is that advection (the left-hand side) is directed along streamlines, while diffusion (the right-hand side) is also perpendicular to the streamlines, along isopotential lines. In high-Reynolds-number fluid mechanics, this is a well known trick due to Boussinesq (1905) still used today, e.g. to describe the advection-diffusion of vorticity (e.g. Hunt & Eames 2002). Streamline coordinates are also used in Maksimov's method for dendritic solidification from a flowing melt (Kornev & Mukhamadullina 1994; Cummings *et al.* 1999). Because Boussinesq's transformation involves interchanging independent and dependent variables, it can also be viewed as a hodographic transformation (Whitham 1974; Ben Amar & Poiré 1999).

Boussinesq's transformation can be viewed as a conformal mapping of the steady, linear advection-diffusion problem to a plane where the flow is uniform. Any obstacles in the flow are mapped to line segments (branch cuts of the inverse map) parallel to the streamlines. For the class of solutions, Eq. (4.7), streamline coordinates correspond to the conformal map,  $f(z) = \sqrt{z}$ , to the upper half plane from a plane of uniform flow past a semi-infinite, absorbing flat plate on the positive real axis (the branch cut), as shown in the top right panel of Fig. 2. In streamline coordinates, therefore, we have the boundary-value problem,

$$\text{Pe} \frac{\partial c}{\partial x} = \nabla^2 c, \quad c(x > 0, 0) = 0, \quad c(-\infty, y) = 1, \quad (4.14)$$

which Carrier *et al.* (1983) solve using the Weiner-Hopf technique. In unpublished lecture notes, H. P. Greenspan solves Eq. (4.14) more easily by introducing parabolic coordinates, motivated by experience with magnetohydrodynamic flows in the same geometry (Greenspan & Carrier 1959; Greenspan 1961), which results in the similarity solution (4.6),

$$\xi = x^2 - y^2, \quad \eta = 2xy, \quad c(x, y) = \text{erf}(\sqrt{\text{Pe}} \eta). \quad (4.15)$$

As explained above, the reason why the similarity ansatz works only becomes clear after conformal mapping to *non*-streamline coordinates in the upper half plane. (See also Cummings *et al.* 1999.)

As this example illustrates, streamline coordinates are not always the most convenient choice, so it is useful to exploit the possibility of conformal mapping to other planes, for both linear and nonlinear advection-diffusion. For similarity solutions, it is much easier to work in a plane where the *diffusive* flux lines, rather than the streamlines, are parallel. Streamline coordinates are also not the best choice in advection-diffusion free boundary problems because stagnation points are associated with branch-point singularities. For flows toward infinite dendrites, it is easier to determine the evolving conformal map from a half plane (Cummings *et al.* 1999). For flows past finite growing objects, it is more convenient to map from the exterior of the unit circle and expand the map in a Laurent series (Shraiman & Bensimon 1984; Hastings & Levitov 1998).

#### (e) Advection-Diffusion Layers Near Leading Edges

Let us consider a few more examples of the similarity solutions in Eq. (4.7). The choice,  $f(z) = \sqrt{z} - a$ , describes a parabolic leading edge,  $x = (y/2\alpha)^2 - \alpha^2$ , where

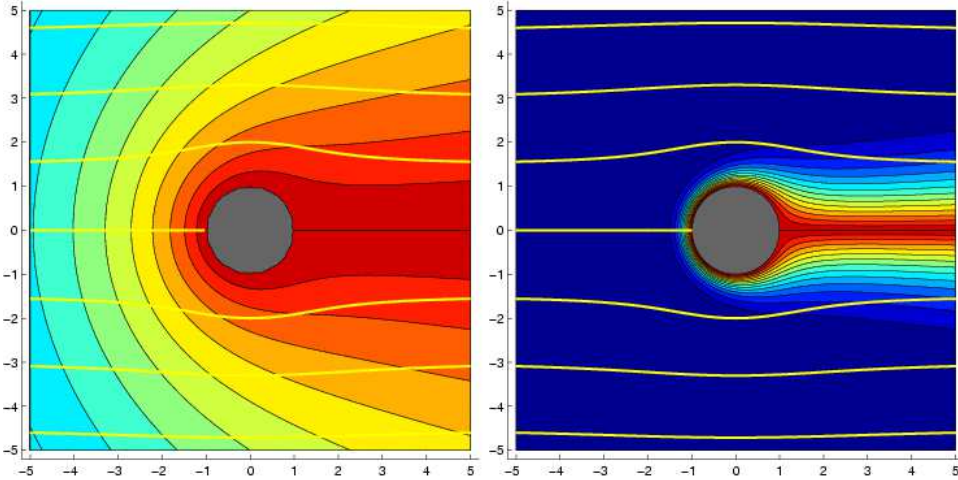


Figure 3. The steady linear advection-diffusion layer around a cylindrical rim on a flat plate at  $\text{Pe} = 0.1$  (left) and  $\text{Pe} = 10$  (right).

$\alpha = \text{Im } a \geq 0$ , as shown in the middle left panel of Fig. 2. This is simply a translation in parabolic coordinates of the flat-plate solution above,  $a = 0$  (Greenspan 1961). For  $\alpha > 0$  the branch point moves off of the boundary, so the solution for a flat wall (rotated by  $\pi/2$ ) is always recovered close to the stagnation point,  $f^{-1}(0)$ .

Another choice,  $f(z) = z^{\pi/(2\pi-\beta)}$ , describes a wedge of opening angle,  $\beta$ , as shown in the middle right panel of Fig. 2 for  $\beta = \pi/2$  (after a rotation by  $\pi/4$ ). The half plate ( $\beta = 0$ ) and the wall ( $\beta = \pi$ ) discussed above are special cases. The diffusive flux on the surface from Eq. (4.12) is singular for acute angles,  $\beta < \pi$ ,

$$|\nabla\phi| \propto \sqrt{\text{Pe}} r^{-\nu}, \quad \nu = \frac{\pi - \beta}{2\pi - \beta}, \quad (4.16)$$

where the geometry-dependent exponent,  $\nu$ , is the same for pure diffusion to the wedge,  $\phi_d \propto \text{Im } f(z)$  (Barenblatt 1995; Redner 2001). This insensitivity to  $\text{Pe}$  is another sign of the conformal equivalence of similarity solutions to Eq. (2.7).

Another interesting example,

$$f(z) = \sqrt{z} + \frac{1}{\sqrt{z}}, \quad (4.17)$$

places a cylindrical rim on the end of a semi-infinite flat plate, as shown in the lower left panel of Fig. 2. The solution has a pleasing form in polar coordinates,

$$\phi = \left( r + \frac{1}{r} \right) \cos \theta \quad (4.18)$$

$$c = \text{erf} \left[ \sqrt{\text{Pe}} \left( \sqrt{r} + \frac{1}{\sqrt{r}} \right) \sin \frac{\theta}{2} \right] \quad (4.19)$$

where we have shifted the velocity potential,

$$\Phi = f(z)^2 - 2 = z + \frac{1}{z}. \quad (4.20)$$

Far from the rim in all directions, we recover the solution for a flat plate, Eq. (4.15), since  $f(z) \sim \sqrt{z}$  as  $|z| \rightarrow \infty$ , but close to the rim, as shown in Fig. 3, there is a nontrivial dependence on  $\text{Pe}$ . For  $\text{Pe} \gg 1$ , a boundary layer of  $O(\text{Pe}^{-1/2})$  thickness forms on the front of the rim and extends to an  $O(\text{Pe}^{-1/2})$  distance from the rear.

The Nusselt number for the total flux to the rim,  $\text{Nu} = 8\sqrt{\text{Pe}/\pi}$ , is mostly easily calculated in the  $w$ -plane where the normal flux is uniform,  $\tilde{F}_w = 2\sqrt{\text{Pe}/\pi}$ , on a line segment of length four (from -2 to 2). Using Eq. (2.10), the distribution of flux density on the surface of the cylinder is readily found to be,

$$\hat{\mathbf{n}} \cdot \nabla c = F_z(|z| = 1) = 2\sqrt{\frac{\text{Pe}}{\pi}} \sin\left(\frac{\theta}{2}\right). \quad (4.21)$$

This is a useful exact result because it also holds for uniform flow past a *finite* absorbing cylinder (not connected to an absorbing flat plate) in the limit of very fast flow,  $\text{Pe} \rightarrow \infty$ , except at  $z = 1$  (the branch point). Since the effect of any disturbance in the concentration decays exponentially upstream beyond a  $O(\text{Pe}^{-1/2})$  distance, adding a plate on the downstream side of the cylinder has no effect in the asymptotic limit,  $\text{Pe} \rightarrow \infty$ , except on the plate itself (the branch cut).

#### (f) Advection-Diffusion Layers Around Finite Objects

It is tempting to try to eliminate the plate from the preceding example by conformal mapping from the exterior of a finite object to the upper half plane. Any such mapping in Eq. (4.7), however, requires a quadrupole point source of flow (mapped to  $\infty$ ) on the object's surface. This is illustrated in the lower right panel of Fig. 2 by a Möbius transformation from the exterior of the unit circle,

$$f(z) = \frac{1+z}{i(1-z)}. \quad (4.22)$$

In this case, a source at  $z = 1$  ejects concentrated fluid in the  $+1$  direction and sucks in fluid along the  $\pm i$  directions.

Thus we see that, due to the boundary conditions at  $\infty$ , uniform flow past an absorbing cylinder (or any other finite object) is in a different family of *non-similarity* solutions, where the diffusive flux lines have a complicated dependence on  $\text{Pe}$ . In streamline coordinates, this includes the problem of uniform flow past a finite absorbing strip, which is equivalent to solving Wijngaarden's transcendental integral equation (Cummings *et al.* 1999). This important family of solutions and its application to free-boundary problems will be described elsewhere.

## 5. Electrochemical Transport

### (a) Dilute Solution Theory

Steady conservation laws (3.1) for gradient-driven fluxes of the form (3.2) also commonly arise in electrochemical systems described by the Nernst-Planck equations (Newman 1991). In this section, we review the complete steady-state equations and boundary conditions, discuss some common approximations which produce conformal invariance, and give some simple, exact solutions. This appears to be the first

application of conformal mapping to *non-Laplacian* electrochemical transport. In certain approximations discussed below, the new technique could be useful in modeling biological and micro-electrochemical systems, where steady states are easily attained due to short diffusion lengths.

In dilute-solution theory, the ionic concentrations,  $\{c_1, c_2, \dots, c_N\}$ , and the electrostatic potential,  $\phi$ , satisfy Eqs. (3.1) and (3.2), where the ‘advection’ velocities,

$$\mathbf{u}_i = -z_i e \mu_i \nabla \phi, \quad (5.1)$$

are due to migration in the electric field ( $\mathbf{E} = -\nabla \phi$ ), where  $e$  is the electron charge,  $z_i$  the charge number (positive or negative) and  $\mu_i$  the mobility of the  $i$ th ionic species. The Einstein-Smoluchowski relation,  $\mu_i = D_i/kT$ , relates the mobility to the diffusivity,  $D_i$ , Boltzmann’s constant,  $k$ , and the temperature,  $T$ . The potential is determined self-consistently by Poisson’s equation,

$$-\nabla \cdot (\varepsilon \nabla \phi) = \rho = \sum_{i=1}^N z_i e c_i \quad (5.2)$$

where  $\varepsilon$  is the permittivity of the solvent and  $\rho$  is the charge density. This equation is not conformally invariant, much like Helmholtz’s equation (1.2), but it is approximately so in most cases of interest (see below).

Scaling concentrations to a reference value,  $C$ , potential to the thermal voltage,  $kT/e$ , length to a typical electrode separation,  $L$ , and assuming constant  $D_i$ ,  $T$ , and  $\varepsilon$ , the  $N + 1$  steady-state equations can be written in the dimensionless form (Bonnefont *et al.* 2001),

$$\nabla^2 c_i + z_i \nabla \cdot (c_i \nabla \phi) = 0, \quad (5.3)$$

and

$$-\epsilon^2 \nabla^2 \phi = \sum_i z_i c_i, \quad (5.4)$$

where  $\epsilon = \lambda/L$  is dimensionless parameter and  $\lambda = \sqrt{\varepsilon kT/e^2 C}$  is the Debye screening length. The dimensionless ionic flux densities and total current density are

$$\mathbf{F}_i = -\nabla c_i - z_i c_i \nabla \phi \quad \text{and} \quad \mathbf{J} = \sum_{i=1}^N z_i \mathbf{F}_i, \quad (5.5)$$

scaled to  $DC/L$  and  $eDC/L$ , respectively.

General boundary conditions on the ionic concentrations express mass conservation. In the case of one active ion ( $i = 1$ ), we have

$$\hat{\mathbf{n}} \cdot \nabla \mathbf{F}_i = \begin{cases} R(c_1, \phi) & \text{for } i = 1 \\ 0 & \text{for } i > 1 \end{cases} \quad (5.6)$$

where  $R(c_i, \phi)$  is a (dimensionless) reaction-rate density for the removal or production of ions at an electrode. It is common to assume Ahrrenius kinetics,

$$R(c_1, \phi) = k_+ c_1 e^{z_1 \alpha_+ (\phi - \phi_e)} - k_- c_e e^{-z_1 \alpha_- (\phi - \phi_e)} \quad (5.7)$$

where  $k_+$  and  $k_-$  are rate constants for deposition and dissolution, respectively (scaled to  $D/L$ ),  $\alpha_{\pm}$  are transfer coefficients,  $c_e$  is the concentration of the neutral

species in the electrode (scaled to  $C$ ) and  $\phi_e$  is the electrode potential (scaled to  $kT/e$ ). In equilibrium ( $R = 0$ ), the potential in the solution at the electrode is given by the (dimensionless) Nernst equation,

$$\phi_{eq} = \phi_e - \frac{\log(kc_1)}{z_1(\alpha_+ + \alpha_-)}, \quad (5.8)$$

where  $k = k_+/k_-c_e$  is an equilibrium constant. Expressing Eq. (5.7) in terms of the ‘surface overpotential’,  $\eta_s = \phi - \phi_{eq}$ , yields the more familiar Butler-Volmer equation (Newman 1991). Equation (5.7) is easily generalized to electrodes which catalyze reactions involving two or more ions, and the mathematical form of the boundary conditions is very similar,

$$\sum_j n_{ij} \hat{\mathbf{n}} \cdot \mathbf{F}_j = R_i(\{c_j\}, \phi), \quad (5.9)$$

where  $\{n_{ij}\}$  are stoichiometric constants. The final boundary condition on the potential can be ignored in neutral electrolytes (see below). When diffuse charge is treated explicitly, a reasonable model accounting for surface capacitance is

$$\phi = \phi_e - \lambda_s \hat{\mathbf{n}} \cdot \nabla \phi \quad (5.10)$$

where  $\lambda_s$  is an effective width for the Stern layer of adsorbed ions (Itskovich *et al.* 1977; Bonnefont *et al.* 2001).

### (b) Approximations and Conformal Mapping

The complete system of nonlinear equations (5.3)–(5.4) and boundary conditions (5.9)–(5.10) are quite complicated, so the theory of electrochemical systems involves a hierarchy of approximations (Newman 1991). In the simplest approximation, the ‘primary current distribution’, the potential satisfies Laplace’s equation, and the ionic concentrations are constants. This can be justified as the linear response of a homogeneous electrolyte to a small applied voltage or current, where Ohm’s Law holds,  $\mathbf{J} = (\sum_{i=1}^N z_i^2 c_i) \mathbf{E} \propto \mathbf{E}$ . It is further assumed that each electrode is an equipotential surface, e.g. given by the Nernst equation (5.8), which is the limit of Eq. (5.6) for ‘fast’ reactions ( $k_+ \gg 1$ ,  $k_-c_e \gg 1$ ). With these assumptions, the potential is simply that of an electrical capacitor, i.e. harmonic with Dirichlet boundary conditions, so standard conformal mapping techniques from electrostatics can be applied (Churchill & Brown 1990; Needham 1997). Indeed, the primary current distribution has been calculated in this way for many electrode geometries in two dimensions (e.g. Moulton 1905; Hine 1956; Newman 1991). All physical effects beyond Ohm’s Law, however, are believed to break conformal invariance, so it seems conformal mapping has not been applied to any more realistic models.

The ‘secondary current distribution’ also assumes a harmonic potential and constant concentrations, but with kinetic boundary conditions, (5.6)–(5.7). In this case, conformal mapping could be of some use. One would need to transform Eq. (5.6) using Eq. (2.10), which introduces a spatially varying coefficient  $|f'|$  in the boundary condition, but one would still solve Laplace’s equation.

A more serious complication is to go beyond Ohm’s law and allow the concentrations to vary according to the Nernst-Planck equations (5.3)–(5.4). Our main

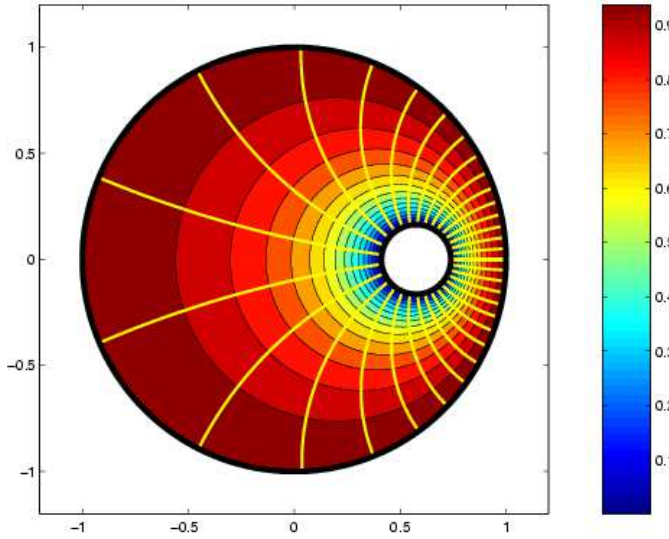


Figure 4. Concentration of an active species (contour plot) and steady current lines (yellow) in a supporting electrolyte between misaligned coaxial, cylindrical electrodes.

insight here is that *the steady mass-conservation equations (5.3) are conformally invariant, for any number of ions*. The Poisson equation, Eq. (5.4), is not conformally invariant, but it turns out that invariance is restored into the usual approximation of either a supporting electrolyte or a quasi-neutral electrolyte. This allows conformal mapping to be applied trivially in the limits of fast reactions and small Stern-layer capacitance (Dirichlet boundary conditions) and with relatively minor complications for the general boundary conditions, Eq. (5.9) and (5.10).

### (c) Concentration of an Active Species in a Supporting Electrolyte

When a large number of inert ‘supporting’ ions are present, charge screening is enhanced, and it is typically assumed that the potential satisfies Laplace’s equation. This can be justified outside diffuse-charge boundary layers (see below), where the other ions are roughly uniform in concentration and neutral overall. In this approximation, the concentration,  $c_1 = c_+$ , of a current-carrying species of charge  $z_+$  obeys Eq. (5.3) with a harmonic potential. The resulting equations,

$$\nabla^2 \phi = 0 \quad \text{and} \quad -z_+ \nabla c_+ \cdot \nabla \phi = \nabla^2 c_+, \quad (5.11)$$

are equivalent to those of linear advection-diffusion in a potential flow, Eq. (4.1) with  $b(c) = 1$ , where the ‘fluid velocity’ is the electric field and the ‘Péclet number’ is  $z_+$ . In this case, the analog of Boussinesq’s transformation would be a mapping to *electric-field coordinates*.

For example, for any electrode configuration,  $0 \leq \operatorname{Re} f(z) \leq 1$ , which can be mapped to a strip,  $0 < \operatorname{Re} w < 1$ , we obtain,  $\phi = \operatorname{Re} f(z)$ , and,

$$c_+ = \frac{1 - e^{-z_+ \operatorname{Re} f(z)}}{1 - e^{-z_+}}, \quad (5.12)$$

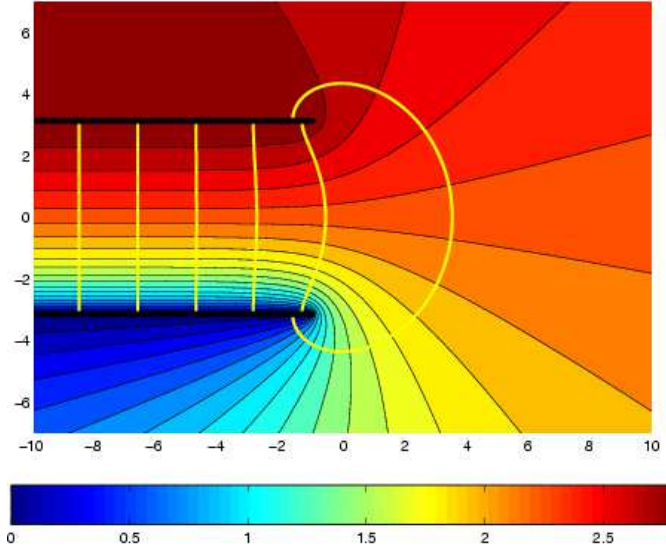


Figure 5. Electrostatic potential (contour plot) and current lines (yellow) in a binary electrolyte between semi-infinite plates at 90% of the limiting current.

for simple Dirichlet boundary conditions:  $c_+ = \phi = 0$  at the cathode,  $\operatorname{Re} f(z) = 0$ , and  $c_+ = \phi = 1$  at the anode,  $\operatorname{Re} f(z) = 1$ . The choice,

$$f(z) = 1 + \log_4 \left( \frac{5z - 3}{5 - 3z} \right), \quad (5.13)$$

which maps to the strip via a Möbius transformation to concentric circles, is illustrated in Fig. 4 for  $z_+ = 1$ . The Equivalence Theorem implies that the current lines and iso-concentration lines are mutually orthogonal circles, as in the case of linear diffusion,  $c_+ = \operatorname{ef}(z)$ , although nonlinearity enhances concentration gradients near the cathode (the inner circle). More generally, *for two equipotential, equiconcentration electrodes in any geometry, the spatial distribution of current along each electrode with a supporting electrolyte is the same as in the primary current distribution*. This is essentially the theorem of Koplik, Redner, and Hinch (1994, 1995) for advection-diffusion discussed above. The special equivalence breaks down, however, for three or more electrodes (or more general boundary conditions).

#### (d) Concentration Polarization in a Neutral Electrolyte

Since the Debye length ( $\lambda \approx 1 - 100\text{nm}$ ) is usually much smaller than the electrode separation ( $\epsilon \ll 1$ ), even in micro-electrochemical systems, it is reasonable to replace Poisson's equation (5.4) by the condition of electroneutrality (Newman 1991),

$$\sum_{i=1}^N z_i c_i = 0 \quad (5.14)$$

which is trivially conformally invariant. This ubiquitous assumption can be firmly justified outside thin boundary layers of 'diffuse charge' using matched asymptotic

expansions (Newman 1965) all the way up to the limiting current (Smyrl & Newman 1967) and beyond (Shtilman & Rubinstein 1979). The effect of the diffuse-charge layers can be incorporated into effective boundary conditions on the bulk, which still have the form of Eq. (5.6), although the Butler-Volmer equation (5.7) acquires a ‘Frumkin correction’ (which is modified somewhat if  $\lambda_s > 0$ ). This is actually the most common perspective in electrochemistry, where the diffuse-charge layer is incorporated with the Stern layer into a single ‘double layer’ (Newman 1991), and the comments above about boundary conditions still apply.

With the conformally invariant equations (5.3) and (5.14), the potential is generally not harmonic (Newman 1991). Instead, it is implicitly determined by charge conservation,  $\nabla \cdot \mathbf{J} = 0$ . The deviation from a harmonic potential with the same boundary conditions, ‘concentration polarization’, is very important at high currents.

As a simple case, consider a neutral binary electrolyte ( $N = 2$ ), where the concentration of positive (or negative) charge,  $c = z_+c_+ = |z_-|c_-$ , and the potential satisfy,

$$\nabla^2 c = 0 \quad \text{and} \quad \nabla \cdot (c \nabla \phi) = 0. \quad (5.15)$$

(The steady concentration is harmonic only for  $N = 2$ .) Assuming that anions are chemically inert yields an invariant zero-flux condition at each electrode,  $\hat{\mathbf{n}} \cdot (\nabla c - c \nabla \phi) = 0$ , and a constraint on the integral of  $c$ , which sets the total number of anions (Bonnefont *et al* 2001). (We rescale  $\phi$  to set  $z_+ = 1$ .) In the limit of fast reactions, the surface potential of the cathode is given by the Nernst equation,  $\phi = -\log kc$ , where  $k$  is an equilibrium constant. The potential at the anode is the cell voltage,  $\phi = V$ .

We obtain a family of similarity solutions for parallel-plate electrodes by conformal mapping,  $w = f(z)$ , to a strip,  $-1 < \text{Im } w < 1$ . The concentration is,  $c = 1 + J \text{Im } f(z)$ , and the potential is,

$$\phi = \log \left( \frac{1 + J \text{Im } f(z)}{k(1 - J)^2} \right), \quad (5.16)$$

where  $J$  is the uniform mapped current density, scaled to the limiting current. At  $J = 1$ , the concentration at the cathode ( $\text{Im } f(z) = -1$ ) vanishes, and the cell voltage,  $V = \phi(\pi) = \log((1 + J)/k(1 - J)^2)$ , diverges due to diffusion limitation.

For example, the classical conformal map (Churchill & Brown 1990),

$$z = f^{-1}(w) = \pi w + e^{\pi w}, \quad (5.17)$$

unfolds our strip like a ‘fan’ to cover the  $z$ -plane and maps the electrodes (twice) onto semi-infinite flat plates ( $\text{Im } z = \pm\pi$ ,  $\text{Re } z < -1$ ). As shown in Fig. 5 for  $J = 0.9$ , this describes the fringe fields of semi-infinite, parallel-plate electrodes. The Equivalence Theorem implies that the current lines are cycloids,  $z_a(\eta) = a + i\eta + e^a e^{i\eta}$ , as in the limit of a harmonic potential at low currents,  $\phi \sim J \text{Im } f(z) - \log k$ . At high currents, the electric field is nonlinearly amplified near the cathode (the lower plate) by concentration polarization. As above, *the spatial distribution of steady current on two equipotential electrodes in a neutral binary electrolyte is the same as in the primary current distribution*, but not for more than two electrodes or more than two ionic species.

## 6. Conclusion

We have observed that certain systems of nonlinear equations involving ‘dot products of two gradients’ are conformally invariant. This has allowed us to extend the classical technique of conformal mapping to some non-harmonic functions of physical interest. A class of examples in transport theory includes steady conservation laws for gradient-driven fluxes.

For one variable, the most general equation in our class (with some well known examples in nonlinear diffusion) can always be reduced to Laplace’s equation. For two or more variables, however, the solutions to our equations are not simply related to harmonic functions, aside from special similarity solutions. By identifying a broad class of equations with the same basic property of conformal invariance, we reveal a geometrical equivalence among different physical transport problems in two dimensions, whose flux lines and iso-concentration lines have universal shapes. This gives physical significance to the property of conformal invariance.

For two variables, there is one example in our class, linear advection-diffusion in a potential flow, to which conformal mapping has been applied extensively. In this case, our method is equivalent to Boussinesq’s streamline coordinates, but somewhat more general. A nonlinear diffusivity is also allowed, and the mapping need not be to a plane of uniform flow (parallel streamlines). In a series of examples, we consider flows past absorbing leading edges mapped to a plane of parallel diffusive-flux lines (and curved streamlines). With these results, we generalize a recent equivalence theorem of Koplik, Redner, and Hinch (1994, 1995).

Our class also contains standard limits of the Nernst-Planck equations for a supporting electrolyte and a quasi-neutral electrolyte. In electrochemistry, conformal mapping has been applied only to harmonic functions, so we present some new results. For example, we find that Ohm’s Law gives the correct spatial distribution of current on any pair of equipotential electrodes in two dimensions, even if the transport is nonlinear and non-Laplacian (but conformally invariant), although this is not true for three or more electrodes. We also calculate the concentration polarization near the edges of two semi-infinite, parallel-plate electrodes.

Although it is beyond the scope of this paper to do so, our results allow conformal mapping to be applied to free boundary problems with non-Laplacian transport equations. In particular, the Polubarnova-Galin (or Shraiman-Bensimon 1984) equation for continuous Laplacian growth (Howison 1992) and the Hastings-Levitov method of iterated conformal maps for stochastic Laplacian growth (Hastings & Levitov 1998) can be extended to any conformally invariant transport (ongoing work with J. Choi and B. Davidovitch). In this way, for example, one can analyze fractal growth by advection-diffusion in a background potential flow, a problem which would otherwise appear to be intractable, even numerically.

The author would like to thank J. Choi for the beautiful, color figures; A. Ajdari, M. Ben Amar, D. Crowdy, B. Davidovitch, I. Eames, H. P. Greenspan, E. J. Hinch, H. K. Moffatt, and A. Toomre for helpful comments on the manuscript; MIT for a junior faculty leave; and ESPCI for hospitality and support through the Paris Sciences Chair.

## References

Ball, R. C. & Somfai, E. 2002 Theory of diffusion controlled growth. *Phys. Rev. Lett.* **89**, art. no. 135503.

Batchelor, G. K. 1967 *An introduction to fluid dynamics*. Cambridge: Cambridge University Press.

Barra, F., Davidovitch, B. & Procaccia, I. 2002a Iterated conformal dynamics and Laplacian growth. *Phys. Rev. E* **65**, art. no. 046144.

Barra, F., Hentschel, H. G. E., Levermann, A. & Procaccia, I. 2002b Quasistatic fractures in brittle media and iterated conformal maps. *Phys. Rev. E* **65**, art. no. 045101.

Barenblatt, G. I. 1995 *Scaling, self-similarity, and intermediate asymptotics*. Cambridge: Cambridge University Press.

Bedia, M. A. & Ben Amar, M. 1994 Investigations of the dendrite problem at zero surface tension in 2D and 3D geometries. *Nonlinearity* **7**, 765–776.

Ben Amar, M. 1991 Exact self-similar shapes in viscous fingering. *Phys. Rev. A* **43**, 5724–5727.

Ben Amar, M. & Brener, E. 1996 Laplacian and diffusional growth: A unified theoretical description for symmetrical and parity-broken patterns. *Physica D* **98**, 128–138.

Ben Amar, M. & Poiré, E. C. 1999 Pushing a non-Newtonian fluid in a Hele-Shaw cell: From fingers to needles. *Phys. Fluids* **11**, 1757–1767.

Bensimon, D., Kadanoff, L. P., Shraiman, B. I. & Tang, C. 1986 Viscous flows in two dimensions *Rev. Mod. Phys.* **58**, 977–999.

Bonnefont, A., Argoul, F., & Bazant, M. Z. 2001 Asymptotic analysis of diffuse-layer effects on time-dependent interfacial kinetics. *J. Electroanal. Chem.* **500**, 52–61.

Boussinesq, M. J. 1905 Sur le pouvoir refroidissant d'un courant liquide ou gazeux. *J. de Math.* **1**, 285–290.

Burgers, J. M. 1948 A mathematical model illustrating the theory of turbulence. *Adv. Appl. Mech.* **1**, 171–199.

Carrier, G., Krook, M., & Pearson, C. E. 1983 *Functions of a complex variable*. Ithaca, New York: Hod Books.

Chan, R. H., Delillo, T. K. & Horn, M. A. 1997 Numerical solution of the biharmonic equation by conformal mapping. *SIAM J. Sci. Comp.* **18**, 1571–1582.

Churchill, R. V. & Brown, J. W. 1990 *Complex variables and applications*, fifth edn. New York: McGraw-Hill.

Cole, J. D. 1951 On a quasilinear parabolic equation occurring in aerodynamics. *Quart. J. Appl. Math.* **9**, 225–236.

Crank, J. 1975 *Mathematics of diffusion*, 2nd edn. Oxford: Clarendon Press.

Crowdy, D. 1999 A note on viscous sintering and quadrature identities. *Eur. J. Appl. Math.* **10**, 623–634.

Crowdy, D. 2002 Exact solutions for the viscous sintering of multiply connected fluid domains. *J. Eng. Math.* **42**, 225–242.

Cummings, L. M., Hohlov, Y. E., Howison, S. D. & Kornev, K. 1999 Two-dimensional solidification and melting in potential flows. *J. Fluid. Mech.* **378**, 1–18.

Dai, W.-S., Kadanoff, L. P. & Zhou, S.-M. 1991 Interface dynamics and the motion of complex singularities. *Phys. Rev. A* **43**, 6672–6682.

Davidovitch, B., Hentschel, H. G. E., Olami, Z., Procaccia, I., Sander, L. M. & Somfai, E. 1999 DLA and iterated conformal maps. *Phys. Rev. E* **59**, 1368–1378.

Davidovitch, B., Feigenbaum, M. J., Hentschel, H. G. E. & Procaccia, I. 2000 Conformal dynamics of fractal growth patterns without randomness. *Phys. Rev. E* **62**, 1706–1715.

Eames, I. & Bush, J. W. M. 1999 Long dispersion by bodies fixed in a potential flow. *Proc. Roy. Soc. A* **455**, 3665–3686.

Feigenbaum, M. J., Procaccia, I. & Davidovitch, B. 2001 Dynamics of finger formation in Laplacian growth without surface tension. *J. Stat. Phys.* **103**, 973–1007.

Galin, L. A. 1945 Unsteady filtration with a free surface. *Dokl. Acad. Nauk. S.S.S.R.* **47**, 2446–249 (in Russian).

Greenspan, H. P. & Carrier, G. F. 1959 The magnetohydrodynamic flow past a flat plate. *J. Fluid Mech.* **6**, 77–96.

Greenspan, H. P. 1961 On the flow of a viscous electrically conducting fluid. *Quart. J. Appl. Math.* **18**, 408–411.

Hastings, M. & Levitov, L. S. 1998 Laplacian growth as one-dimensional turbulence. *Physica D* **116**, 244–252.

Hastings, M. B. 2001 Fractal to nonfractal phase transition in the Dielectric Breakdown Model. *Phys. Rev. Lett.* **87**, art. no. 175502.

Henrici, P. 1986 *Applied and computational complex analysis*, vol. 3. New York: Wiley.

Hine, F., Yoshizawa, S. & Okada, S. 1956 Effects of walls of electrolytic cells on current distribution. *J. Electrochem. Soc.* **103**, 186–193.

Hopf, E. 1950 The partial differential equation  $u_t + uu_x = \mu u_{xx}$ . *Comm. Pure Appl. Math.* **3**, 201–230.

Howison, S. D. 1986 Fingering in Hele-Shaw cells. *J. Fluid Mech.* **167**, 439–453.

Howison, S. D. 1992 Complex variable methods in Hele-Shaw moving boundary problems. *Euro. J. Appl. Math.* **3**, 209–224.

Hunt, J. C. R. & Eames, I. 2002 The disappearance of laminar and turbulent wakes in complex flows. *J. Fluid Mech.* **457**, 111–132.

Itskovich, E. M., Kornyshev, A. A. & Vorotyntsev, M. A. (1977) Electric current across the metal-solid electrolyte interface (I): Direct current, current-voltage characteristic. *Phys. Stat. Sol. (a)* **39**, 229–238.

Ivantsov, G. P. 1947 *Dokl. Akad. Nauk. S.S.S.R.* **58**, 567 (in Russian).

Kardar, M., Parisi, G. & Zhang, Y.-C. 1986 Dynamic scaling of growing interfaces. *Phys. Rev. Lett.* **56**, 889–892.

Kessler, D. A., Koplik, J. & Levine, H. 1988 Pattern selection in fingered growth phenomena. *Adv. Phys.* **37**, 255–339.

Kimura, S. & Bejan, A. 1983 The ‘heatline’ visualization of convective heat transfer. *AMSE J. Heat Transfer* **105**, 916–919.

Kirchhoff, G. 1984 *Vorlesungen über die theorie der wärme*. Leipzig: Barth.

Koplik, J., Redner, S. & Hinch, E. J. 1994 Tracer dispersion in planar multipole flows. *Phys. Rev. E* **50**, 4650–4667.

Koplik, J., Redner, S. & Hinch, E. J. 1995 Universal and nonuniversal first-passage properties of planar multipole flows. *Phys. Rev. Lett.* **74**, 82–85.

Kornev, K. & Mukhamadullina, G. 1994 Mathematical theory of freezing for flow in porous media. *Proc. Roy. Soc. London A* **447**, 281–297.

Leal, G. 1992 *Laminar flow and convective transport processes*. New York: Butterworth-Heinemann.

Medina, E., Hwa, T., Kardar, M. & Zhang, Y.-C. 1989 Burgers equation with correlated noise: RG analysis and applications to directed polymers and interface growth. *Phys. Rev. A* **39**, 3053–3075.

Moulton, H. F. 1905 Current flow in rectangular conductors. *Proc. London Math. Soc. (ser. 2)* **3**, 104–110.

Morega, M. & Bejan, A. 1994 Heatline visualization of forced convection in porous media. *Int. J. Heat Fluid Flow* **36**, 42–47.

Morse, P. M. & Feshbach, H. 1953 *Methods of theoretical physics*. New York: McGraw-Hill.

Muskhelishvili, N. I. 1953 *Some basic problems in the mathematical theory of elasticity*. Groningen, Netherlands: Noordhoff.

Needham, T. 1997 *Visual complex analysis*. Oxford: Clarendon Press.

Newman, J. 1965 The polarized diffuse double layer. *Trans. Faraday Soc.* **61**, 2229–2237.

Newman, J. 1991 *Electrochemical systems*, 2nd. edn. Englewood Cliffs, NJ: Prentice-Hall.

Niemeyer, L., Pietronero, L. & Wiesmann, H. J. 1984 *Phys. Rev. Lett.* **52**, 1033–1036.

Polubarinova-Kochina, P. Ya. 1945a *Dokl. Akad. Nauk. S.S.R.* **47**, 254–257 (in Russian).

Polubarinova-Kochina, P. Ya. 1945b *Prikl. Matem. Mech.* **9**, 79–90 (in Russian).

Redner, S. 2001 *A guide to first-passage processes*. Cambridge: Cambridge University Press.

Rubinstein, I. & Shtilman, K. 1979 Voltage against current curves of cation exchange membranes. *J. Chem. Soc. Faraday Trans. II* **75**, 231–246.

Saffman, P. G. 1986 Viscous fingering in Hele-Shaw cells. *J. Fluid Mech.* **173**, 73–94.

Saffman, P. G. & Taylor, G. I. 1958 The penetration of a fluid into a porous medium or Hele-Shaw cell containing a more viscous liquid. *Proc. R. Soc. London A* **245**, 312–329.

Sen, M. & Yang, K. T. 2000 Laplace's equation for convective scalar transport in potential flow. *Proc. Roy. Soc. Lond. A* **456**, 3041–3045.

Shraiman, B. I. & Bensimon, D. 1984 Singularities in nonlocal interface dynamics. *Phys. Rev. A* **30**, 2840–2842.

Smyrl, W. H. & Newman, J. 1967 Double-layer structure at the limiting current. *Trans. Faraday Soc.* **63**, 207–216.

Somfai, E., Sander, L. M. & Ball, R. C. 1999 Scaling and crossovers in diffusion aggregation. *Phys. Rev. Lett.* **83**, 5523–5526.

Stepanov, M. G. & Levitov, L. S. 2001 Laplacian growth with separately controlled noise and anisotropy. *Phys. Rev. E* **63**, art. no. 061102.

Tanveer, S. 1987 Analytical theory for the selection of a symmetrical Saffman-Taylor finger in a Hele-Shaw cell. *Phys. Fluids* **30**, 1589–1605.

Tanveer, S. 1993 Evolution of Hele-Shaw interface for small surface tension. *Phil. Trans. R. Soc. London A* **343**, 155–204.

Trefethen, L. N. 1986 *Numerical conformal mapping*. Amsterdam: North Holland.

Whitham, G. B. 1974 *Linear and nonlinear waves*. New York: Wiley.

Witten, T. A. & Sander, L. M. 1981 Diffusion-limited aggregation: A kinetic critical phenomenon. *Phys. Rev. Lett.* **47**, 1400–1403.